DEUTSCHES ELEKTRONEN – SYNCHROTRON

DESY 92-095
July 1992

— A —

Direct and Resolved Photon Contribution to Inelastic ep Scattering. W^+ Production at HERA: A Case Study.

F. M. Borzumati

II. Institut für Theoretische Physik, Universität Hamburg

ISSN 0418-9833

NOTKESTRASSE 85 · D-2000 HAMBURG 52

ISSN 0418-9833

DESY 92-095
July 92

Direct and Resolved Photon Contribution to Inelastic *ep* Scattering. W^+ Production at HERA: A Case Study. *

Francesca M. Borzumati

II. Institut für Theoretische Physik †
Universität Hamburg, D - 2000 Hamburg 50

ABSTRACT

We investigate the problem of matching direct and resolved photon contributions to hard *ep* scattering at high energies. In order to avoid double counting, a suitable subtraction mechanism has to be used throughout the full range of virtuality of the exchanged photon. We illustrate our procedure of summing direct and resolved photon contributions in the specific case of W^+ production at HERA.

*Talk given at the Zeuthen Workshop on Elementary Particle Physics "Deep Inelastic Scattering", Teupitz, Germany, April 6–10, 1992.

†Supported by the Bundesministerium für Forschung und Technologie, 05 4HH 92P/3, Bonn, FRG.

To be published in:
Nuclear Physics B (Proc. Suppl.)
North-Holland

DIRECT AND RESOLVED PHOTON CONTRIBUTIONS TO INELASTIC *EP* SCATTERING. W^+ PRODUCTION AT HERA: A CASE STUDY.

Francesca M. Borzumati

II. Institut für Theoretische Physik, Universität Hamburg, D - 2000 Hamburg 50

Supported by the Bundesministerium für Forschung und Technologie, 05 4HH 92P/3, Bonn, FRG.

We investigate the problem of matching direct and resolved photon contributions to hard *ep* scattering at high energies. In order to avoid double counting, a suitable subtraction mechanism has to be used throughout the full range of virtuality of the exchanged photon. We illustrate our procedure of summing direct and resolved photon contributions in the specific case of W^+ production at HERA.

1. Introduction

The class of *ep* processes subject of this talk is the rather large class of processes dominated by the exchange of a single photon. At the HERA energy, an enormous range in the photon virtuality (P^2) will be probed, ranging from approximately $s = 10^5\,\mathrm{GeV}^2$ down to almost zero. The problem of matching the so-called **direct** and **resolved** photon contributions to these processes has then to be addressed i) in the case of photoproduction ($P^2 = 0$) cross sections or low-P^2 *ep* cross sections, ii) in the case of P^2-integrated *ep* cross sections. A clear recipe to handle the former case has been proposed in ref. [1] and used also in [2]. In both references, though, it was extended to the case of P^2-integrated cross sections.

The aim of this talk is to present a working strategy for the calculation of photon mediated *ep* cross sections where the problem of matching direct and resolved photon contributions arises. We closely follow ref. [3]. The strategy proposed applies to all the above mentioned *ep* reactions. Some numerical results are discussed in the specific case of W^+bosons production where the matching problem arises at the leading order in α_S, in contrast to other cases (as in jets production) where the matching is required in the next to leading order.

2. The matching problem

We immediately restrict ourselves to the photon mediated subprocess

$$\gamma^*(p) + p(p_p) \rightarrow q(k) + X(p_X) \tag{1}$$

of the generic process

$$e(l) + p(p_p) \rightarrow e(l') + q(k) + X(p_X)\;. \tag{2}$$

In the case of W^+ production, X is the W^+ boson plus the proton remnant. The Feynman diagrams contributing to (1) are shown for this case in Fig. 1. In what follows we use s to denote the center of mass (CM) energy squared, $s = (l + p_p)^2$ and W^2 for the γp CM energy squared, $W^2 = (p + p_p)^2$.

For massless quarks, the cross sections for the processes (2) are dominated by two large logarithmic integrations. One logarithm originates

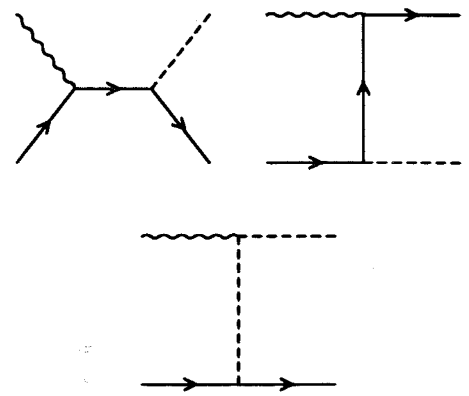

Fig. 1. Direct-photon-exchange diagrams contributing to W^+ production. The wavy, dashed and continuous lines indicate photons, W bosons and quarks, respectively.

from the propagator of the exchanged photon, $P^2 = -p^2 = -(l-l')^2$. The other one stems from the propagator of the light quark in the u-channel, $u = (p_p - p_X)^2$. The differential cross sections for the reactions (2) have in general the form:

$$\frac{d\,\sigma_{ep}[\text{direct}]}{d\,W^2} = \frac{1}{(W^2)^2}\int_{P^2_{\rm min}}^{P^2_{\rm max}} \frac{dP^2}{P^2}\int_{|u|_{\rm min}}^{|u|_{\rm max}}\frac{d|u|}{|u|} \left\{A + B\,\frac{W^2}{W^2+P^2} + C\,\frac{|u|}{W^2}+\ldots\right\} \qquad (3)$$

where A, B, C etc. are functions independent of P^2 and u. At small P^2 and $|u|$ the term A is the dominant one, while at large values of the photon virtuality P^2 and/or of the variable $|u|$ the non-leading terms proportional to B, C, ... in (3) become important and may even exceed the logarithmic terms.

In the interesting case $m_p^2 \ll W^2 \ll s$ and $P^2 \ll W^2$ the integration limits are given by

$$m_e^2\left(\frac{W^2}{s}\right)^2 \le P^2 \le s - W^2 \qquad (4)$$

$$P^2 \sim P^2\,\frac{m_X^2}{W^2} \le |u| \le W^2 - m_X^2 + P^2 \,. \qquad (5)$$

The scale for the cross section Q^2, is typically given by W^2. A closer inspection of (3) allows the following observations:

– The u-integration $\int du/u$ yields a potentially large term $\log\left(Q^2/P^2\right)$. For values of P^2 small enough, the lower integration limit $|u|_{\rm min}$ can become much smaller than the QCD scale parameter Λ. This indicates the limit of applicability of a purely perturbative calculation.

– The large term $\log\left(Q^2/P^2\right)$ gets contributions from any order in the strong coupling α_S. Multiple gluon radiation brings in a series of extra quark propagators. Each of them yields such a logarithmic term compensating the additional powers of α_S due to the new gluon-quark-antiquark vertex ($\alpha_S(Q^2)\log(Q^2) = \mathcal{O}(1)$).

This brings us immediately to the discussion of the resolved photon contribution. The correct summation of direct and resolved contribution, in fact, enables us to deal with these two problematic aspects of the direct contribution.

The resolved photon contribution is given in terms of the **photon structure function** [4] (**PHSF**). Working in a physical gauge, the PHSF can be shown to be the sum of the so-called ladder diagrams, starting with a pointlike $\gamma q q$ vertex or a hadronic input. On the other hand, the direct cross section contains all the Feynman diagrams of the order in α_S at which one is working. Thus, certain terms of the direct cross section are already included in the PHSF. We denote them as σ_{ep}[dir-sing] since they are the terms responsible for the $|u|$-pole in (3), while we indicate the remaining ones by σ_{ep}[dir-fin]. In order to avoid double counting, σ_{ep}[dir-sing] must be subtracted from the simple sum of σ_{ep}[direct] and σ_{ep}[resolved]. This roughly amounts to dropping the term A in (3), except for a small remainder which we call σ_{ep}[rest], due to the mismatch in

the kinematic of the direct and resolved contributions.

The total cross section is in principle then given by the sum

$$\sigma_{ep}[\text{total}] = \sigma_{ep}[\text{dir-fin}] + \sigma_{ep}[\text{resolved}] + \sigma_{ep}[\text{rest}] \,. \qquad (6)$$

The resolved photon cross section σ_{ep}[resolved] resums the potentially large terms $\log(Q^2/P^2)$ contributing to the cross section at every order in α_S. It deals with the problem of singular integrations over regions of too small values of $|u|$ and P^2, encountered in the evaluation of σ_{ep}[dir-sing], by the use of data taken from experiments.

The procedure displayed in (6) (proposed in [1] for the case of W production) would be the complete answer to the matching problem if the PHSF would be known as functions of P^2 over the range that is needed at HERA, i.e. from $P^2 \ll \Lambda^2$ up to $P^2 \sim 10^5\,\text{GeV}^2$. In practice we can numerically deal only with the so-called region of the **real PHSF** with $P^2 \ll \Lambda^2 \ll Q^2$, and of the **virtual PHSF** with $\Lambda^2 \ll P^2 \ll Q^2$. Several parametrizations exist for the real PHSF and moreover, the analytic expression of the virtual PHSF in moment space, is also known. Two more regions of P^2, besides the ones already mentioned, are involved in the calculation of photon mediated ep processes: $P^2 \sim \Lambda^2 \ll Q^2$ and $\Lambda^2 \ll P^2 \sim Q^2$. It is intuitive that for high enough values of P^2, i.e. for $P^2 \sim Q^2$, the **quark parton model (QPM)** result should give a valid description of the PHSF. In contrast, the continuation of the real and virtual solution over the region $P^2 = \mathcal{O}(\Lambda^2)$ is non-trivial.

We show in Fig. 2 the P^2 dependence of the known solutions for the singlet distribution function $\Sigma^\gamma(n, Q^2, P^2)$ for different moments n. At the leading order in α_S, $\Sigma^\gamma(n, Q^2, P^2)$ can be ex-

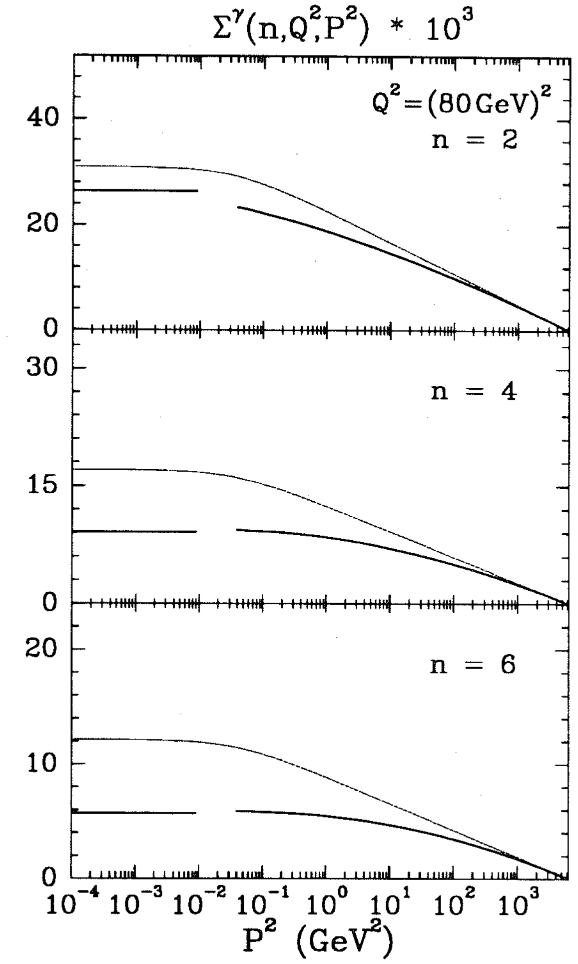

Fig. 2. Comparison of the virtual singlet solution (decreasing thick line), with the lowest order result for $\Sigma^\gamma(n, Q^2, P^2)$ (faint upper line) and the value of the real singlet distribution (straight thick line) as given by the LAC1 parametrization for $n_f = 4$ and $\Lambda = 0.2$ GeV.

pressed in terms of the distributions of the quark and anti-quark in the photon as

$$\Sigma^\gamma(n, Q^2, P^2) = \sum_i \left[q_i^\gamma(n, Q^2, P^2) + \bar{q}_i^\gamma(n, Q^2, P^2)\right] \,. \qquad (7)$$

In Fig. 2 the virtual solution has been extrapolated down to Λ^2 and the real one, as obtained from the LAC1 parametrization [5], is extended up to $(10^{-1}\,\mathrm{GeV})^2$. The lowest order approximation to $\Sigma^\gamma(n,Q^2,P^2)$, i.e. the QPM result with the logarithmic term continued to $\log(Q^2/(P^2{+}\Lambda^2))$, exhibits a very slow onset of a P^2 dependence and a smooth behaviour over the region $P^2 \sim \Lambda^2$. The same features are observed also when higher twists corrections are added to the QPM result [3]. This suggests that a matching of the real and virtual distribution functions can be reasonably performed. The precise value of P, which we call P_{cut}, depends clearly on n, Q^2 and the particular real PHSF parametrization used.

The singlet distribution function can then be approximated over the full range of P^2 by:

$$\Sigma^\gamma(n,Q^2,P^2) = \Sigma^{\gamma\ \mathrm{REAL}}(n,Q^2)\theta(P^2_{cut}-P^2) + \Sigma^{\gamma\ \mathrm{VIRT}}(n,Q^2,P^2)\ \theta(P^2-P^2_{cut})\ . \quad (8)$$

The distribution (8) and analogous ones for $q_i^\gamma(n,Q^2,P^2)$ and $\overline{q}_i^\gamma(n,Q^2,P^2)$ can be used to evaluate σ_{ep}[resolved], once an inversion to x space is performed. For the time being, a simplified expression can be obtained if the QPM approximation to the virtual PHSF is used. We expect to obtain in this way slightly overestimated values for the total and differential cross sections.

The total cross section can still be cast in the form (6) if the following identification is made:

$$\begin{aligned}\sigma_{ep}[\text{dir-fin}] &= \sigma_{ep}^{\mathrm{REAL}}[\text{dir-fin}]+\sigma_{ep}^{\mathrm{VIRT}}[\text{dir-fin}]\\ \sigma_{ep}[\text{resolved}] &= \sigma_{ep}^{\mathrm{REAL}}[\text{resolved}]+\sigma_{ep}^{\mathrm{VIRT}}[\text{dir-sing}]\\ \sigma_{ep}[\text{rest}] &= \sigma_{ep}^{\mathrm{REAL}}[\text{rest}]\ . \end{aligned} \quad (9)$$

The superscripts REAL and VIRT in (9) indicate that the P^2 integration has been carried out from P^2_{min} to P^2_{cut} and from P^2_{cut} to P^2_{max}, respectively. Moreover, the real PHSF enters in $\sigma_{ep}^{\mathrm{REAL}}$[resolved] while $\sigma_{ep}^{\mathrm{VIRT}}$[resolved] is approximated by $\sigma_{ep}^{\mathrm{VIRT}}$[dir-sing].

The same procedure can be followed in the calculation of differential cross sections.

3. Numerical Results for W^+ Production

The results presented in this section are obtained by using the EHLQ [6] parametrization for the distribution of the quark in the proton. The arbitrary scales present in the proton and in the photon distribution functions are both set to M_W. The Weizsäcker-Williams approximation [7] is also used and finally the value of P_{cut} is taken equal to the mass of the ρ meson. In Fig. 3 we show the W^+ rapidity distribution for $\sqrt{s} = 314\,\mathrm{GeV}$ and $1.8\,\mathrm{TeV}$ in the ep CM reference frame, as obtained by following the procedure described in the previous section. The positive and negative direction in the plots in Fig. 3 are the electron and the proton beam directions, respectively. A shift of $(1/2)\ \log(E_e/E_p)$ in the x-positive direction, allows to read the rapidity distribution in the laboratory frame.

In both cases $d\sigma_{ep}[\text{dir-fin}]/dy$ is highly peaked towards positive values of rapidity. Of the different contributions to $d\sigma_{ep}[\text{resolved}]/dy$ we show $d\sigma_{ep}^{\mathrm{REAL}}[\text{resolved}]/dy$ in the DG [8] and LAC1 [5] parametrizations and in the QPM approximation. We observe how the use of different parametrizations introduces quite a big uncertainty giving distributions more or less peaked at negative values of the rapidity. The contribution $d\sigma_{ep}^{\mathrm{VIRT}}[\text{dir-sing}]/dy$ has on the contrary the same shape as the QPM result in the region of P^2 between $P_{\min}$ and P_{cut}. The difference is simply due to the different P^2 integration regions involved in the two cases. We expect smaller values for the resolved contribution in the region between P_{cut} and $P_{\max}$ and, possibly, the disappearence of the peak in the positive direction when the expression for the virtual photon structure func-

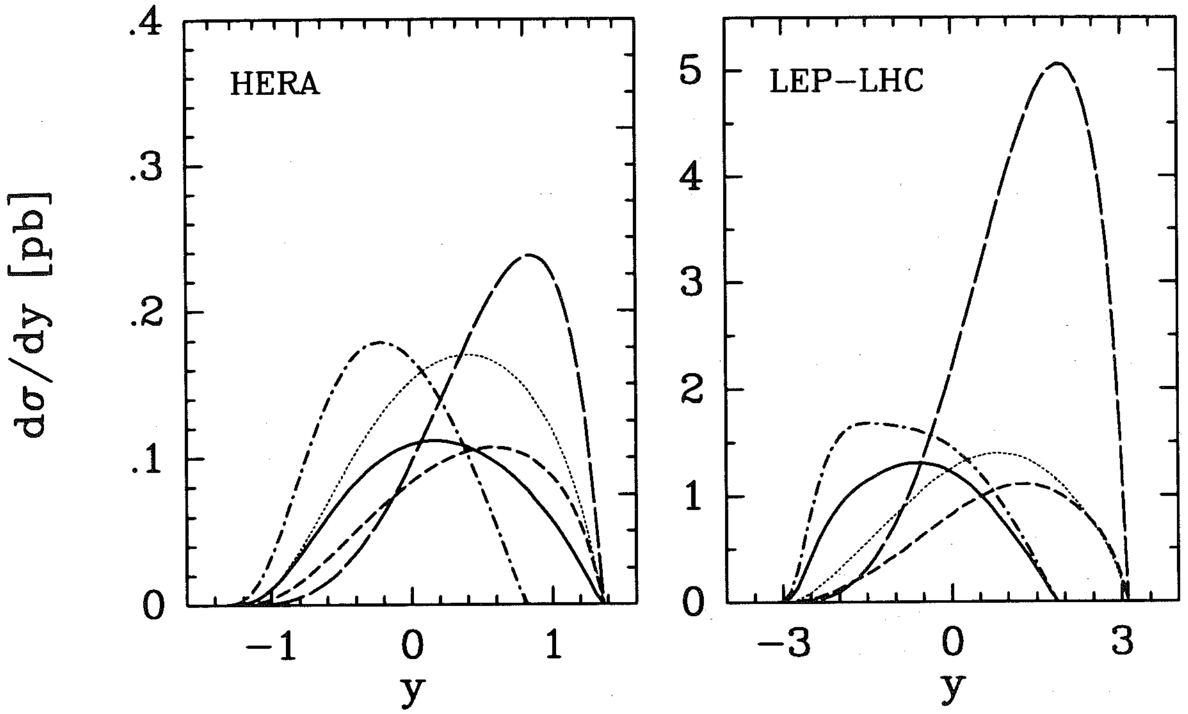

Fig. 3. Rapidity distribution of W^+ at ep CM energies of 314 GeV (a) and 1.8 TeV (b). The long-dashed curve is the sum of the finite part of the direct contributions above and below the P^2 cut, while the short-dashed one is the singular part of the direct contribution above the same cut. The solid, dot-dashed and dotted lines are the resolved contribution below the P^2 cut, obtained using the DG and LAC1 parametrization for the PHSF and the QPM approximation, respectively.

tion is actually used. The big difference in shape between the contributions to $d\sigma_{ep}[\text{resolved}]/dy$ and $d\sigma_{ep}[\text{dir-fin}]/dy$ shows clearly that the proposal of deriving the total rapidity distribution through a scaling of the resolved photon distribution by a constant K factor [2] is not acceptable.

As can be seen from Table 1, the same uncertainty observed in the rapidity distribution, due to the use of different real PHSF parametrizations, is present also in the results for the total cross section. It can reach values up to 50% and 30% in $\sigma_{ep}^{\mathrm{REAL}}$[resolv] for $\sqrt{s} = 314\,\mathrm{GeV}$ and $1.8\,\mathrm{TeV}$, respectively. The uncertainty is sensibly diluted to the values of 18% and 8% for the same CM energies when all the contributions are summed together to give σ_{ep}[total].

The values shown in Table 1 for the total cross section should be compared with the results obtained when the subtraction (6) is extended to the ep cross section P^2-integrated from $P^2_{\min}$ to $P^2_{\max}$. For $\sqrt{s} = 314\,\mathrm{GeV}$, we obtain the value of 0.53, 0.70 and 0.71 if the DG, LAC1 and LAC2 parametrizations are used. In the case of $\sqrt{s} = 1.8\,\mathrm{TeV}$, the results are 23.1, 26.4 and 26.7 respectively. As could be already observed from Fig. 2, the extension of the real PHSF throughout the full range of P^2 leads to an overestimation of the cross section, at least when the LAC1 parametrization is used. However, the effect is less than 10%, i.e. it does not exceed the uncer-

	σ_{ep}[dir-fin]	$\sigma_{ep}^{\mathrm{REAL}}$[resolv] DG, LAC1, LAC2	$\sigma_{ep}^{\mathrm{VIRT}}$[dir-sing]	$\sigma_{ep}^{\mathrm{REAL}}$[rest]	σ_{ep}[total] DG, LAC1, LAC2
HERA	0.27	0.18, 0.27, 0.28	0.16	-0.029	0.58, 0.68, 0.69
LEP ⊗ LHC	13.7	5.0, 6.8, 7.0	3.7	0.12	22.6, 24.4, 24.6

Table 1
Different contributions to the total cross section

tainty due to the arbitrariness of the scale in the PHSF [1].

We conclude now with a quick comparison of our procedure to the one presented in ref. [9]. Even there the phase space integration is divided in two regions. In one, where small values of the u variable are involved, the scheme (6) is applied, while only the full direct contribution is considered elsewhere. The distinction of the two regions is performed through a cut in the variable u. Real PHSF parametrizations are then used in the evaluation of the resolved photon contribution also for large values of P^2 below the u cut. The numerical results, however, are similar to the ones we obtain.

4. Conclusions

In spite of the smallness of the effects of different matching procedure in the case of W^+ production, we believe that the key point in this type of calculations should be the correct treatment of the structure of the photon in its range of virtuality. One would like to achieve a smooth continuation of the virtual PHSF into the real one. In particular, this continuation might help in selecting among the existing real PHSF parametrizations, therefore reducing the main uncertainty in the evaluation of photon mediated ep cross sections.

Acknowledgements

I thank G.A. Schuler for a pleasant collaboration and J. Blümlein for participating in an early stage of the work presented here.

References

[1] J. Blümlein and G. Schuler, IfH-Zeuthen preprint, PHE 90-21, (1990).
[2] C.S. Kim and W.J. Stirling, *Z. Phys.* **C53** (1992) 601.
[3] F.M. Borzumati and G.A. Schuler, DESY preprint, DESY 92-078, CERN-6519/92, MPI-Ph/91-113, (1992).
[4] Due to lack of space, we refer the reader to [3] and the references therein reported.
[5] H. Abramowicz, K. Charchula and A. Levy, *Phys. Lett.* **B269** (1991) 458.
[6] E. Eichten, I. Hinchliffe, K. Lane and C. Quigg, *Rev. Mod. Phys.* **56** (1984) 579, (E) *ibid.* **58** (1986) 1065.
[7] C.F. Weizsäcker, Zeit. für Physik **88** (1934) 612; E.J. Williams, Phys. Rev. **45** (1934) 729.
[8] M. Drees and K. Grassie, *Z. Phys.* **C28** (1985) 451.
[9] U. Baur, J.A.M. Vermaseren and D. Zeppenfeld, *Nucl. Phys.* **B375** (1992) 3.